ChemCatChem

The European Society Journal for Catalysis

Chemistry Europe

European Chemical Societies Publishing

Supported by

GECATS GERMAN CATALYSIS SOCIETY

Accepted Article

Title: Time-resolved DRIFT spectroscopy study of carbonaceous intermediates during the water gas shift reaction over Au/ceria catalyst

Authors: Julia Vecchietti, Gustavo Belletti, Paola Quaino, Adrian Bonivardi, and Sebastian Collins

To be cited as: *ChemCatChem* **2023**, e202300435

Link to VoR: https://doi.org/10.1002/cctc.202300435

WILEY VCH

10.1002/cctc.202300435

Time-resolved DRIFT spectroscopy study of carbonaceous intermediates during the water gas shift reaction over Au/ceria catalyst

Julia Vecchietti[a], Gustavo Belletti[b,c], Paola Quaino[b,c], Adrian Bonivardi[a,c], Sebastián Collins[a,c,*]

[a] Instituto de Desarrollo Tecnológico para la Industria Química (INTEC), Universidad Nacional del Litoral and CONICET, Güemes 3450, 3000, Santa Fe, Argentina.

[b] Instituto de Química Aplicada del Litoral (IQAL), Universidad Nacional del Litoral and CONICET, Santiago del Estero 2829, 3000, Santa Fe, Argentina.

[c] Facultad de Ingeniería Química, Universidad Nacional del Litoral, Santiago del Estero 2829, 3000, Santa Fe, Argentina.

***Corresponding author**: scollins@santafe-conicet.gov.ar

Authors' full name, ORCID, e-mail

Julia Vecchietti, ORCID 0000-0001-7672-3027 jvecchietti@santafe-conicet.gov.ar

Paola Quaino, ORCID 0000-0003-1311-5213, pquaino@fiq.unl.edu.ar

Gustavo Belletti, ORCID 0000-0001-8466-7897, gbelletti@fiq.unl.edu.ar

Adrian Bonivardi, ORCID 0000-0002-8575-675X, abonivar@santafe-conicet.gov.ar

Sebastián E. Collins, ORCID 0000-0002-2157-3305, scollins@santafe-conicet.gov.ar

10.1002/cctc.202300435

Abstract

The mechanism of the low-temperature water gas shift reaction (LTWGS) on an Au/CeO_2 catalyst was investigated by means of in situ diffuse reflectance infrared (DRIFT) spectroscopy. Under steady-state LTWGS reaction (373-623 K), the catalyst is partially reduced, and signals from carbonate/formate dominates the infrared spectra. Time-resolved pulse of CO experiment under a constant partial pressure of water at 423 K indicates that Ce^{4+} can be reduced to Ce^{3+} and that formate (HCOO) species cannot be directly related to the CO_2 production. Further information was obtained by performing modulation excitation spectroscopy (MES) experiments coupled with a phase-sensitive detection (PSD) method. Under periodic modulation of the CO partial pressure while keeping the H_2O concentration constant, most of the intense bands of carbonate and formate remained constant, indicating that these species are only spectators. The same is observed for the concentration of Ce^{+3}. Conversely, signals in-phase with the conversion of CO to CO_2 are observed and assigned to carboxyl [C(O)OH] and carboxylate ($CO_2^{\delta-}$) species, while some monodentate formate (m-HCOO) also changes but at a lower rate. A plausible associative reaction mechanism where carboxyl/carboxylate are key intermediates is postulated.

INTRODUCTION

The water gas shift (WGS) reaction, followed by the preferential oxidation of CO, is crucial for the production of high-purity hydrogen with less than 50 ppm of CO in order to achieve an efficient operation of the polymer electrolyte membrane (PEM) fuel cells. Since the WGS reaction is equilibrium limited and moderately exothermic ($CO + H_2O \rightarrow H_2 + CO_2$ ΔH^0 = -41 kJ/mol), active catalysts at temperatures as low as 423 K are needed to reach those very low CO concentration levels [1]. It has been proposed that gold nanoparticles dispersed on reducible oxides such as titanium [2] and cerium oxides [3], constitute the most promising and highly efficient catalyst system for the low temperature WGS (LT-WGS) reaction.

In particular, special emphasis has been placed on the metal-support interface to carry out that reaction. It has been highlighted that the size, shape and exposed crystal plane of ceria regulate the structure of the metal–support interfaces, which in turn control the reaction rate [3–6]. This hypothesis is based on intensive experimental and theoretical simulations studies on powder and model M/CeO_2 catalysts systems [4,7–9]. However, direct evidence under working condition on the chemical nature of the true reaction intermediates in the Au/CeO_2 system is still scare.

Two reaction mechanisms have been proposed in the literature, involving the metal–support interfaces in ceria-supported precious metal catalyst: (i) the redox mechanism, where CO is adsorbed on metal sites and reacts with a lattice oxygen atom from the support to produce CO_2, subsequently the generated oxygen vacancy is replenished by water and hydrogen is released [10–12]; and, (ii) the associative mechanism where different reaction intermediates are proposed, including formate (HCOO) [12–16], carbonate (CO_3) [17,18] or carboxyl [C(O)OH]/carboxylate ($CO_2^{\delta-}$) [9,19–22]. In the case of the associative mechanism, carboxyl species was first theoretically proposed [9,23], but only indirect evidence has been experimentally shown on model catalyst [22] and, more recently on a powder Pd/Al_2O_3 catalysts for the reverse-WGS [24].

A comprehensive understanding of the WGS mechanism at molecular-level is critical for the design of more efficient catalytic materials. In this context, investigations of heterogeneous catalysis employ a diverse range of spectroscopic methods, among which vibrational spectroscopies, especially infrared spectroscopy, hold prominence due to their versatility and extensive use. IR techniques can be employed in situ and operando, enabling the acquisition of information about the catalytic reaction mechanism. However, the signals from the actual active species are typically weak and strongly overlapped with the signals of spectator species not engaged in the catalytic surface processes. For selective extraction of information on active species, transient spectroscopic techniques have been developed, such as, pulse-reaction, steady-state isotopic transient kinetic analysis (SSITKA) [25,26]

and, more recently, modulation excitation spectroscopy (MES) [27,28]. MES operates under quasi-steady-state conditions forced by periodic perturbation of the system by changing an external parameter, e.g. concentration, temperature, irradiation, or pH. This transient method facilitates selective detection of surface molecules responding to an external perturbation, enhancement of the signal-to noise (S/N) ratio and extraction of kinetic information by phase sensitive detection (PSD) [27].

In this work, the reaction mechanism of LT-WGS on a gold-ceria catalyst is investigated using DRIFT spectroscopy under steady-state, pulse-reaction and modulated (MES-PSD) experiments, and complementary DFT calculations. Direct evidence on the role of key reaction intermediates are presented.

RESULTS AND DISCUSSION

WGS reaction

Table 1 summarizes the main features and the WGS activity of CeO_2 and Au/CeO_2 catalysts. As is shown in Table 1, deposition–precipitation with urea was an efficient method for the preparation of the Au/CeO_2 catalyst, achieving a gold loading close to the nominal value and a high metal dispersion of 68% (see Figure S1). Au/CeO_2 presented a high WGS reaction activity, reaching the equilibrium conversion at ca. 523 K. The dispersion of gold remained almost constant after the reaction as determined by TEM. Conversion curve as a function of temperature is presented in Figure S2.

Table 1. Characterization and WGS activity of CeO_2 and Au/CeO_2

Characterization	CeO_2	Au/CeO_2
Au (wt%)	-	1.87
S_{BET} (m^2/g)	62	57
D (%)[a]	-	68 (57)[b]
WGS activity[c]		
T (K)		r_{CO} ($cm^3/g/h$)
373	-	90
423	-	395
473	-	880
523	63	1054

WGS activity of other Au/CeO_2 catalysts reported in the literature

Catalysts	Feed composition	Temperature (K)	r_{CO} ($cm^3/g/h$)	Ref.
2.6%Au/CeO_2	1%CO; 2%H_2O	453	887	[29]
4.75% Au/CeO_2	2% CO; 10.7% H_2O	473	296	[30]
2% Au/CeO_2		523	48	[31]

2% Au/$CeZrO_4$	2% CO; 2.5% CO_2; 7.5% H_2O; 8.1% H_2	448	720	[29]
4.5%Au/CeO_2	1%CO; 2%H_2O	453	1306	[29]
0.5%Au/CeO_2	2%CO; 8%H_2O	393	114	[32]

[a] Metal dispersion by TEM

[b] Metal dispersion post WGS activity measurement

[c] Conditions: 1% CO + 2% H_2O balanced with He (total flow = 100 cm^3/min), 50 mg of catalyst.

WGS reaction under steady state monitored by DRIFT spectroscopy

The water gas shift reaction was studied under steady state condition over the Au/CeO_2 catalyst using DRIFT spectroscopy. Figure 1 shows the collected spectra after 1 h of exposure to the reaction mixture (1%CO +2% H_2O) at each temperature between 373 and 623 K. For comparison, infrared spectrum under He before introduction of the WGS mixture is also included.

Exposure to the reaction mixture at 373 K promotes the formation of a large number of bands associated with different carbonates and formate species on the support, and CO adsorbed on Au sites. Bands assigned to different types of formate species (HCOO) bound to the ceria support are observed: ν(CH) = 2830 cm^{-1}, the combination modes δ(CH)+ ν_{as}(COO) = 2945 cm^{-1} and δ(CH)+ ν_s(COO) = 2711 cm^{-1}, ν_{as}(COO) = 1580,1550 cm^{-1}, ν_s(COO) = 1336 and δ(CH) = 1370 cm^{-1} [33,34]. Broad and ill resolved bands are also developed in the 1700-1200 cm^{-1} region, which can be ascribe to carbonate groups [35,36].

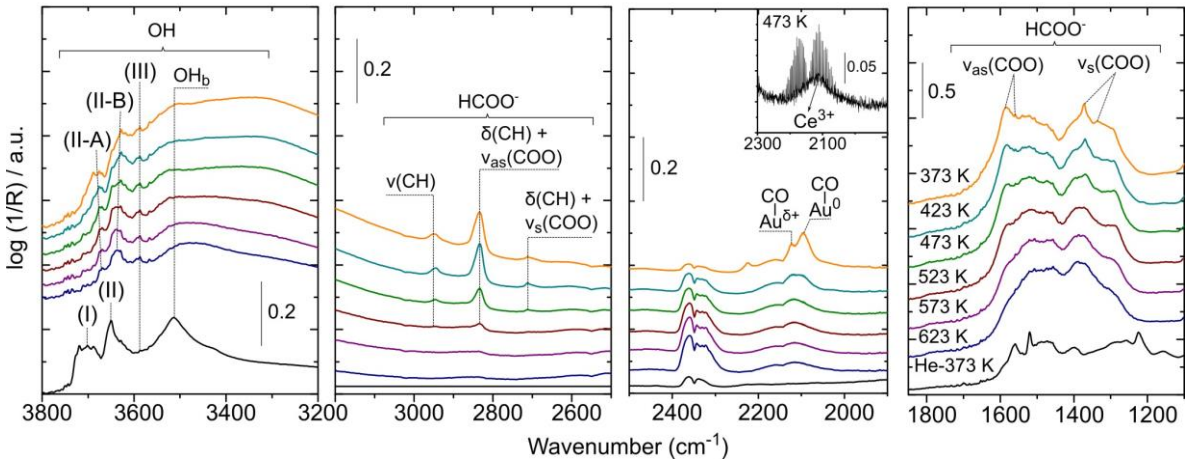

Figure 1. DRIFT spectra taken after 1 h of exposure to the reaction mixture (1%CO + 2%H_2O) over Au/CeO_2 catalyst between 373 and 623 K. The bottom spectrum was taken under He at 373 K before exposure to the reaction mixture.

In the region between 2500-1900 cm^{-1} the bands associated with CO adsorbed on $Au^{\delta+}$ and Au^0 sites are observed at 2120 and 2096 cm^{-1}, respectively [37–42]. These carbonyl species show up at the lowest temperature tested, and their intensities decrease as the temperature raises, disappearing at 473 K (Figure 2). A complementary spectrum collected at a resolution of 0.5 cm^{-1} (inset Figure 1) allows to differentiate among the rotovibrational signals of gas phase CO from the broad signal at ca. 2125 cm^{-1} due to the presence of Ce^{3+} reduced surface sites (forbidden electronic transition $^2F_{5/2} \rightarrow {}^2F_{7/2}$) [43,44] at 473K.

In the OH region of the spectra, important changes occur due to the exposure to the WGS reaction mixture. Before reaction, characteristic bands are observed at 3705, 3658, 3590 and 3510 cm^{-1} assigned to linear, OH(I), two-fold bridged, OH(II), thee-fold bridged OH(III), and hydrogen-bonding hydroxyls, OH_b, or oxyhydroxy species on the oxidized ceria surface (Ce^{+4} sites) [45]. After the introduction of the reaction mixture at 373 K, the OH(I) band disappears and new signals appear at 3676 and 3634 cm^{-1} due to the partial reduction of the support, giving rise to type II-A and II-B OH species, respectively, bonded to Ce^{+3} sites [43,45]. Additionally, a very broad band from 3600 to 3000 cm^{-1} markedly increased due to the adsorption of water on the support, which at high coverage produces broadening of the ν(OH) stretching mode, due to hydrogen bonding.

Figure 2 shows the integrated absorbance of selected signals. As the temperature rises, an increase of the band at ~ 2350 cm^{-1} of gaseous CO_2 is observed as a consequence of the progress of the reaction. Simultaneously, bands due to formate species and CO bound to gold decrease as the reaction temperature increases. On the other hand, integration of the carbonate region between 1550 and 1385 cm^{-1}, where there is no overlap with formate bands, shows that the coverage of the carbonate groups grows with increasing reaction temperature.

DRIFT spectra collected under steady state during the water gas shift reaction clearly show that OH, CO, carbonate and formate species are formed and their coverage changes as the reaction temperature is increased. Additionally, partial reduction of the support is observed. However, the role of these surface species (or others undetected under these experimental conditions) as reaction intermediates or spectators is not clear. In order to detect the species that could be involved in the reaction, dynamic (transient) experiments were carried out.

Pulse experiments monitored by time-resolved DRIFT spectroscopy

A time-resolved CO pulse study, while keeping the partial pressure of water constant, was performed by DRIFT spectroscopy. The experiments were carried out at 423 K, that is, at approximately 30% of CO conversion (see Figure S2), to allow a balance between the formation and consumption rates

10.1002/cctc.202300435

of the intermediates in order to achieve a sufficient surface concentration of such species to be detected by IR. Thus, the Au/CeO_2 catalyst was exposed to a flow of $2\%H_2O$/He at 423 K, allowed to stabilize, and then a pulse of 5%CO (elapsed time = 10 s) was introduced while keeping the partial pressure of water constant ($5\%CO+2\%H_2O$/He). During a period of 50 seconds, spectra were taken in rapid scan mode, at a velocity of 2.6 spectra/second. Figure 3 shows, as an example, a few of the DRIFTS spectra taken during and after the CO pulse, subtracted from the one collected before the pulse. Figure 4 presents the time-evolution of selected IR signals.

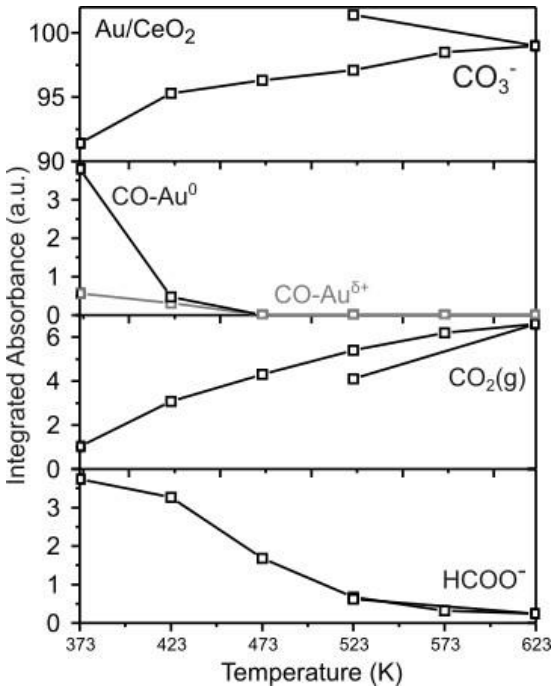

Figure 2. Thermal evolution of the intensity of the IR bands during the WGS reaction for the Au/CeO_2 catalyst under the reaction mixture (1% CO + 2% H_2O).

It is worth noting that there is a short delay between the CO(g) and CO_2(g) traces (Figure 4), indicating that even at 423 K, the WGS reaction proceeds at a high rate. After the end of the CO(g) pulse, the signal of Ce^{3+} remains in the spectra, proving that the catalyst was reduced by CO, even under the constant partial pressure of water. For a better visualization, the spectra after subtraction of gas-phase CO are shown in the inset of Figure 3. The increase of the Ce^{3+} signal (Fig. 4) is in the same time-frame than CO and CO_2 signals, showing that the subtraction of oxygen from the ceria lattice is very fast. The IR bands of adsorbed CO on Au are not registered or are overlapped with the CO gas during the pulse. In any case, after the pulse no Au-CO species were observed.

10.1002/cctc.202300435

During the introduction of CO pulse, a fast accumulation of carbon-containing species in the 1900-1100 cm^{-1} region of the spectra is also observed. The integrated area of the region between 1565-1300 cm^{-1} as a function of time shows that the formate/carbonate species grew and its concentration remained constant after the end of the CO pulse. Nevertheless, it is difficult to extract information from this spectral zone due to the overlapping among the high intensity carbonate bands and other (smaller) IR bands due, for example, to formate species.

A small band at 2826 cm^{-1} and a pair of bands at 1590 and 1370 cm^{-1} assigned to formate species are also detected. As shown in Figure 4, the evolution of the 2826 cm^{-1} IR signal, which is free of overlapping with others IR bands, depicts that formate species slowly accumulates on the catalyst surface, after the partial reduction of the ceria surface. This result suggests that Ce^{3+} species might be necessary in order to stabilize formate groups in the surface of the support, and/or that formate stabilizes Ce^{3+}. This last suggestion is consistent with the constant IR signal of Ce^{3+} after the CO pulse (t > 30 s).

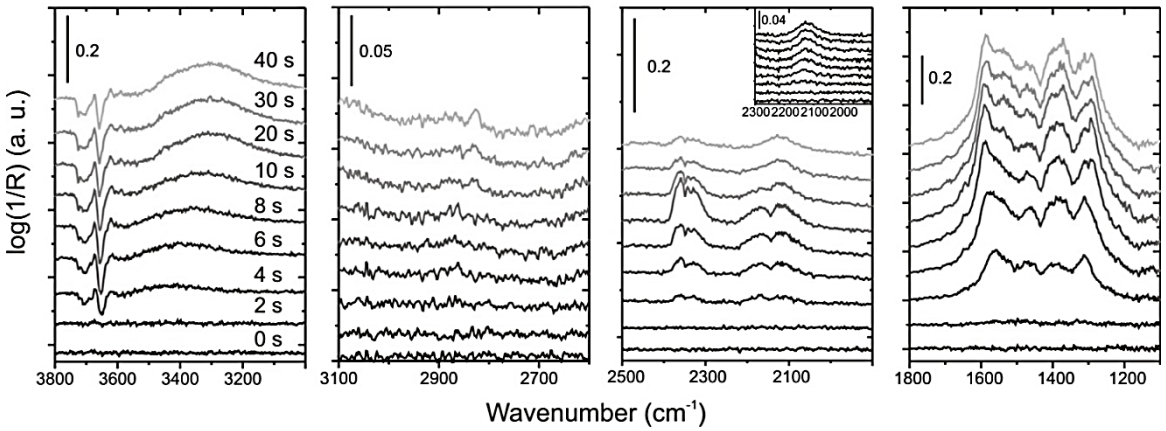

Figure 3. DRIFT spectra taken during and after 5%CO pulse (elapsed time = 10 s) study on the Au/CeO_2 catalyst at 423 K. Water concentration (2%H_2O) was kept constant throughout the experiment. The inset shows the Ce^{3+} signal after subtraction of gas phase CO.

Interestingly, in the ν(OH) stretching region, the negative bands at 3705 and 3658 cm^{-1} assigned to OH type I and II on Ce^{4+} are an indication of consumption of these OH specie during the CO pulse (Figure 4). On the other hand, although the concentration of water remains constant, the wide band in the 3400-3200 cm^{-1} developed with the time of exposure to CO (g). The wide OH band initially centred at 3400 cm^{-1} grows and shifts toward lower wavenumbers, and after the CO pulse, stabilized at 3300 cm^{-1}. These results are in agreement with the reduction of Ce^{4+} to Ce^{3+} during the experiment, described above. A complementary experiment of isothermal oxidation with water of the reduced

Au/CeO_2 catalyst by DRIFTS (Figure S3), showed that the oxidation of Ce^{3+} to Ce^{4+} is not complete. In fact, only 30% of the Ce^{3+} was re-oxidized by water. For comparison, Figure S3 also shows the evolution of the Ce^{3+} signal after exposure of the sample to an O_2 current. Clearly the oxidation of Ce^{3+} to Ce^{4+} was complete under O_2 flow and faster when compared to oxidation by water. The difficult oxidation of Ce^{3+} by water was reported in the literature [44] and it is in agreement with the results observed during the CO pulse experiment.

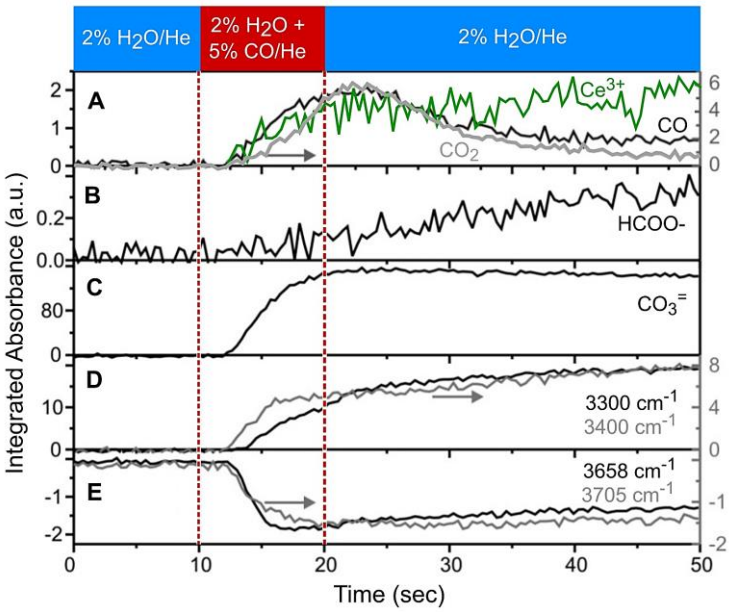

Figure 4. Temporal evolution of the DRIFT signals during the CO pulse experiments at 423 K over Au/CeO_2. The elapsed time of the pulse is marked by the red dotted lines. Formate species were followed by integrating de 2826 cm^{-1} IR signal, while carbonates species were integrated in the region between the 1565-1300 cm^{-1}. CO and CO_2 evolutions were measured at 2170-2130 and 2350 cm^{-1}, while Ce^{3+} was follow at 2125 cm^{-1} after subtracting of the gas phase CO signal.

Furthermore, the time evolution of the DRIFT bands during the CO pulse suggests that the formation of formate species is not correlated with the production of CO_2 during the transient period of the reaction over Au/CeO_2 catalyst. That is, formate surface species accumulate after the end of the CO pulse, while CO_2 is released a few seconds after the introduction of CO into the DRIFT cell reaching a maximum at the end of the CO pulse. However, at this point it cannot be ruled out that another type of more reactive formate species may exist, which decomposes (to yield CO_2) faster than its formation, hindering its detection. Additionally, this pulse experiment was performed over the oxidized surface of the support, which was different to the one under steady state WGS reaction

conditions, that is, where the ceria surface was partially reduced. Then, it cannot be excluded the involvement of other formate species under WGS reaction conditions.

Overall, the CO pulse experiments allowed us to obtain information about the possible role of some of the surface species present during the WGS reaction. Particularly, the reduction of the support by CO, even under constant H_2O pressure was observed. The production of CO_2 seems to be related with this last process, but the direct involvement of formate species in the CO_2 production is not clear. Even more, the rapid accumulation of carbonates in the finger-print region hamper the selective identification of possible carbonaceous intermediates of the water gas shift reaction. Therefore, to bring light to this point on the reaction mechanism, in other words, to further detect intermediates that can be actually involved under steady state of the WGS reaction, concentration modulated experiments (c-MES) experiments were performed.

Modulation excitation DRIFT spectroscopy

These experiments were carried out keeping constant the partial pressure of water by switching from a 2%H_2O/He flow to the reaction mixture of 1%CO + 2%H_2O/He with a frequency equal to 8.3 mHz (T = 2 min) at 423 K. Figure 5 shows the time domain spectra at 0 and 60 s (half period for clarity) in the top panel and the phase domain spectra obtained at selected phase lag of 20, 200 and 300° after applying PSD algorithm. Figure S4 shows the 2-D iso-intensity maps spectra as a function of the phase lag (ϕ^{PSD}).

As before, in the steady-state and pulse experiments, time-resolved spectra during the c-MES experiment are highly complex in the 1800-1000 cm^{-1} region, due to intense and overlapped signals. These very intense bands only slightly change with the modulation. However, phase-resolved spectra after applying the PSD algorithm, allow a better observation of the spectral changes (see Table 2 for the detailed assignment of the most significant IR bands detected in the phase resolved spectra). In the time-resolved spectra, most of the broad and intense peaks at ca. 1525, 1400, and 1310 cm^{-1} remain almost constant during the modulated experiment, as a consequence they are "filtered" in the phase-resolved spectra. That indicates that the carbonates (CO_3^{-2}) bounded to the ceria are spectators. A similar behaviour is observed for the peaks at 2944, 2831, and 2712 cm^{-1}, indicating that this type of formate species are not reacting and remain as spectator species. It must be noted that this piece of information is provided by MES-PSD experiments [28]. Burch and collaborators arrived to similar conclusions by *in situ* quantitative DRIFTS experiments over high activity WGS catalysts (Pt/ZrO_2, $Au/Ce(La)O_2$, Pt/CeO_2 and $Au/CeZrO_4$) [33,34].

In the OH region, peaks at 3624 and 3583 cm^{-1} assigned to OH type II-A and III are in-phase with CO partial pressure, indicating that they are perturbed or react with CO. While the OH type I, II and II-B at ca. 3690 cm^{-1}, 3676 and 3647 cm^{-1} are out-of-phase with the presence of CO, which can be interpreted as a replenishment of OH consumed/perturbed in the previous cycle by the CO.

Phase-resolved spectra also allow the identification of a series of bands that synchronically changes. The set of bands at 1565, 1370, and 1358 cm^{-1} assigned to the ν_{as}(COO) stretching, the δ(CH) bending and the ν_s(COO) stretching of formate (HCOO) species, respectively, with a phase lag, ϕ^{PSD} = 265° are clearly observed. These infrared peaks are also in-phase with the signals at 2945, 2830 and 2710 cm^{-1} corresponding to the δ(CH)+ν_{as}(COO) combination, ν(CH) stretching mode and δ(CH)+ν_s(COO) combination mode of formate species, which corroborate the assignation to formate species. The position and Δν [ν_{as}(COO) - ν_s(COO)] = 207 cm^{-1}, allows to assign these set of bands to monodentate formate species (m-HCOO) coordinated to one Ce^{3+} and stabilized by adjacent OH groups [33]. Another pair of bands synchronically changes at 1583 and 1335 cm^{-1} with characteristic phase-lag at ϕ^{PSD} = 278°. These couple of bands could be assigned to the ν_{as}(COO) and the ν_s(COO) stretching mode, respectively, of another type of monodentate formate species, coordinated with Ce^{3+} and 3 OH species [33].

Table 2. Experimental frequencies of assigned surface species.

IR mode	**m-HCOO**	**$CO_2^{\delta-}$**	**C(O)OH experimental**	**C(O)OH DFT**
ν(OH)			3245	3524
δ(CH)+ν_{as}(COO)	2945			
ν(CH)	2830			
δ(CH)+ν_s(COO)	2710			
ν_{as}(COO)	1565,1583	1605	1650	1660
δ(CH)	1370			
ν_{as}(COO	1358,1335	1280		
δ(OH)			1210	1210

In the ν(CO) stretching region, the periodic change of the reactant and product of reaction, CO (ϕ^{PSD} = 305°) and CO_2 (ϕ^{PSD} = 315°) is observed. The spectra after subtraction of gas phase CO (blue lines) reveals the presence of two small bands assigned to CO adsorbed on gold (Au-CO) at 2096 and 2120

cm^{-1} (Au$^{\delta+}$-CO and Au^{o}-CO, respectively). Additionally, in the time domain spectra, the presence Ce^{3+} signal is detected. However, after PSD algorithm is applied, the Ce^{3+} signal disappears, which means that the redox state of the ceria support does not change during the modulation of reactants. This is in agreement with what was reported before for Pt/CeO_2 catalysts, suggesting that the redox mechanism is not the main reaction pathway for the LT-WGS reaction [46].

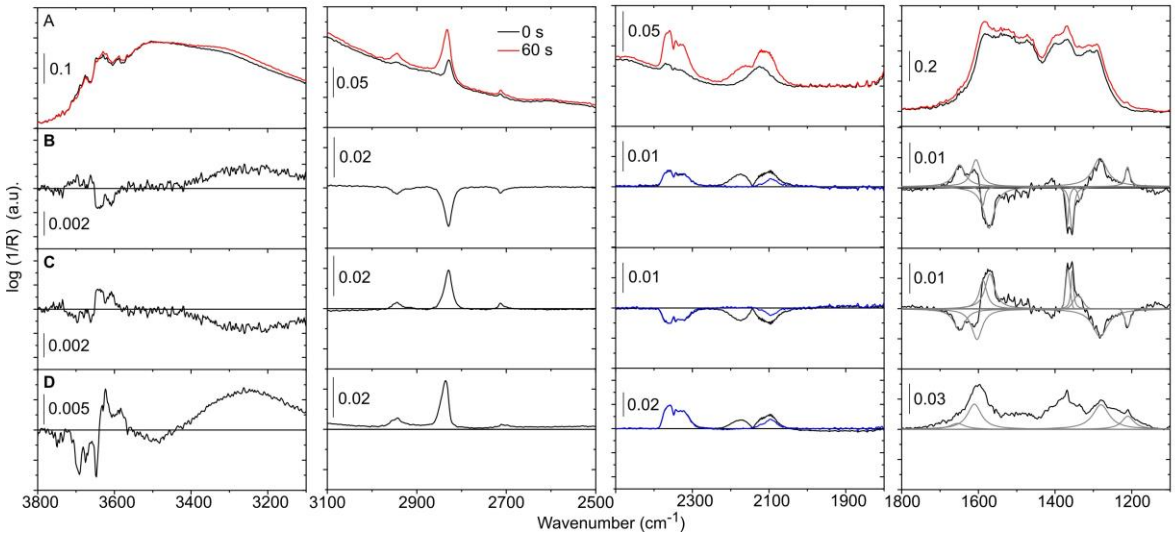

Figure 5. Time domain spectra at 0 and 60 seconds (A) and the phase domain spectra obtained at an angle 20° (B), 200° (C) and 300° (D) after applying PSD algorithm. In the 2500-1800 cm^{-1} region, the spectra after subtraction of gas phase CO is also represented (blue lines). Additionally, in the ν(OCO) region, the deconvolution of the phase-domain spectra is shown (grey lines).

It is worth noting that CO_2 production occurs faster (lower phase lag) than the production of formate (HCOO), which indicates that the formate is not participating in the production of CO_2 or is a slower route. Furthermore, two pair of bands with almost the same phase-lag (ϕ^{PSD} = 305°) are detected at 1650 and 1210 cm^{-1} and 1605, and 1280 cm^{-1}, both of them are in-phase with the production of CO_2. (see Figure S5 for more details). Based on the position and splitting of the bands at 1605 and 1280 cm^{-1} ($\Delta\nu \sim 325$ cm^{-1}), they are ascribed to carboxylate species ($CO_2^{\delta-}$) [14,47,48]. Similar species were detected on Pt/CeO_2 catalyst [46]. The peaks located at 1650 and 1210 cm^{-1} are also in-phase with the broad band at 3250 cm^{-1}, indicating that they belong to the same surface species.

Very recently, Meunier and collaborators reported the formation of a band at 1660 cm^{-1} during CO adsorption over zirconia-supported Pt [49]. This band was assigned to a Pt_2–CO bridging carbonyl interacting head-on with a support surface hydroxyl. This adduct was unstable and converted into a linear and bridged carbonyl bound only to Pt, while at the same time, H-bonded hydroxyls were

quantitatively converted into free hydroxyls. However, as mentioned above, the band observed here at 1650 cm^{-1} changes synchronically with the bands at 1210 and 3250 cm^{-1}, which excludes the assignation to carbonyl species.

Thus, another possible assignation would be a carboxyl intermediate [C(O)OH] [24]. The associative carboxyl mechanism was theoretically proposed [9,23]. However, up to date, scarce spectroscopic evidence for the elusive carboxyl intermediate exists in the WGS literature mainly because of the highly overlapped carbonate/formate spectral zone together with a low intensity and low stability of such a carboxyl species. For instance, a small IR peak at 1242 cm^{-1} was assigned as a possible hydroxycarbonyl intermediate on Au/TiO_2 during CO oxidation reaction [50]. Metallocarboxyl, M-C(O)OH, has been synthetized in gas phase a result of the reaction of metal hydrides with CO_2 [51–53], showing infrared bands of the ν(C=O) mode at 1610-20cm^{-1}. Gas-phase HOCO trapped in a Ne matrix showed signals at 3628, 1848, and 1210 cm^{-1} [54]. Additionally, DFT calculations on Au(110) and Pt(111) predicts the COOH vibrational frequencies at 1680-1670 cm^{-1} and 1230-1260 cm^{-1}, corresponding to the ν(CO) and δ(OH) modes, respectively [55].

In order to further corroborate the band assignation, a complementary DTF calculation of a model carboxyl group at the $Au/CeO_2(111)$ interface was performed (Figure S6). The calculated vibrational modes are: ν(CO) = 1660 cm^{-1}, δ(OH) = 1110 cm^{-1}, ν(OH) = 3524 cm^{-1}. Then, the experimentally phase-resolved bands at 3250, 1650, 1210 cm^{-1} are assigned to the carboxyl species, possible bounded at the metal-support interface.

LT-WGS reaction mechanism

The role of different carbonaceous species, such as formate and carboxyl/carboxylate species, in the WGS reaction mechanism, is still a matter of debate [13,18,34]. The carboxyl mechanism for the WGS reaction was theoretically predicted [9,23]. Nevertheless, carboxylate species have been proposed as an indirect probe of the presence of a carboxyl species [C(O)OH], but those carboxylate has only been detected on single crystals model catalysts [22,56] and, to the best of our knowledge, no direct observation of carboxyl species has been reported yet [24]. The difficulties in detecting carboxyl species arise from the strong peak intensities of spectator carbonate/formate groups, which are always present in the same IR spectral region.

In the present study, which employs in situ DRIFT spectroscopy under steady-state water gas shift reaction on an Au/CeO_2 catalyst, it is showed that CO is adsorbed on metal sites, and formate and carbonate species dominate the spectral features, while ceria is partially reduced (Ce^{3+}) under the reaction condition. At increasing temperatures, the coverage of CO on gold (Au-CO) and of formate

species decrease, while carbonates accumulate as CO_2 production increases. However, it is clear that misinformation can be obtained by observing only the production of surface species, as no differentiation can be made between true reaction intermediates and spectators.

Time-resolved DRIFT spectroscopy during CO pulses under constant water partial pressure on the oxidized Au/CeO_2 catalyst provides further information. It was observed that under isothermal conditions (423 K), the CO is absorbed on the support as carbonates (very intense bands are formed), and also reduces Ce^{+4} to Ce^{3+}, producing CO_2, while formate groups (HCOO) accumulate on the surface at a lower rate, indicating a slower reaction route. Nevertheless, broad and intense bands, particularly in the fingerprint region (1900-1000 cm^{-1}), prevent the identification of others possible carbonaceous intermediates.

Thus, isothermal c-MES experiments were carried out modulating the CO partial pressure while keeping the water partial pressure constant, to provide selective spectroscopic information. It is important to notice that WGS reaction was produced during the cycles, as shown by the emergence of CO_2 when CO in introduced into the cell (Fig. 5). Moreover, after stabilization of the cycles, the ceria support remained partially reduced (band at 2130 cm^{-1}). Phase-resolved spectra indicated that the electronic ($^2F_{5/2} \rightarrow {}^2F_{7/2}$) signal of Ce^{3+} was not affected by the modulation, as it was filtered from the spectra. This is an important result, since the reoxidation of Ce^{3+} to Ce^{4+} by water only proceed partially under H_2O flow (Figure S3). Then, it is proposed that the redox mechanism, involving the reversible $Ce^{3+} \leftarrow \rightarrow Ce^{4+}$ cycle, is not operating on the Au/CeO_2 catalyst at LT-WGS reaction conditions. However, this mechanism could be could be significant at high temperatures, as reported previously [11].

The use of phase-resolved spectra enables the resolution of infrared signals in the 1900-1000 cm^{-1} fingerprint region, providing critical information. Firstly, signals from carbonate were eliminated in the phase-resolved spectra, indicating that these species act as spectators of the reaction. Secondly, it was observed that monodentate formate (m-HCOO) species, possibly bonded to surface Ce^{3+}, proceed via a slower route, as the phase lag was larger than the production of CO_2.

In addition, bands assigned to carboxylate ($CO_2^{\delta-}$) and carboxyl [C(O)OH] species were identified in-phase with the production of CO_2. The IR band assignation to carboxyl species was confirmed by complementary DFT calculations. These elusive reaction intermediates have been theoretically predicted as key WGS reaction intermediates [9,23]. However, direct observation of these species by IR spectroscopy has not been possible with the traditional techniques (e.g., time-resolved, pulse) due to the highly overlapped bands in this spectral region.

All this spectroscopic evidence can be summarized in the reaction mechanism proposed in Scheme 1. Initially, CO adsorbs onto gold sites and reacts with OH at the metal-support interface to form the carboxyl intermediate, [C(O)OH]. Those OH species are provided by water that dissociates at the ceria-gold interface with a low activation barrier (0.64 eV) [9]. CO pulse and c-MES experiments clearly indicate that monodentate formate (m-HCOO) is also formed and consumed during the LT-WGS reaction on Au/CeO_2, but it proceeds through a minor or slower route. Chen et al. [9] and Aranifard et al. [23] proposed that carboxyl and m-HCOO species can be reversibly isomerized at the metal-support interface. So, it seems reasonable that under periodic variation of the CO concentration, m-HCOO acts as a pool of carbonaceous species that can further react, through C(O)OH, to produce CO_2 once the CO concentration stopped.

At this point, it is important to highlight the crucial role of the Au-CeO_2 interface. A complementary experiment of temperature-programmed surface reaction with CO (TPSR-CO) was performed over CeO_2 and Au/CeO_2 (Figure S7). There, the thermal evolution of m-HCOO species showed that the production of this species on pure CeO_2 is delayed almost 200 K as compared with the supported-gold catalyst. Then, as reported previously, the metal-support interface plays a central role in the CO activation in the LT-WGS reaction.

Following the main reaction steps, carboxyl is transformed into carboxylate by losing a hydrogen atom, which recombines with an H from water (or OH) to release a hydrogen molecule. Finally, carboxylate desorbs as CO_2.

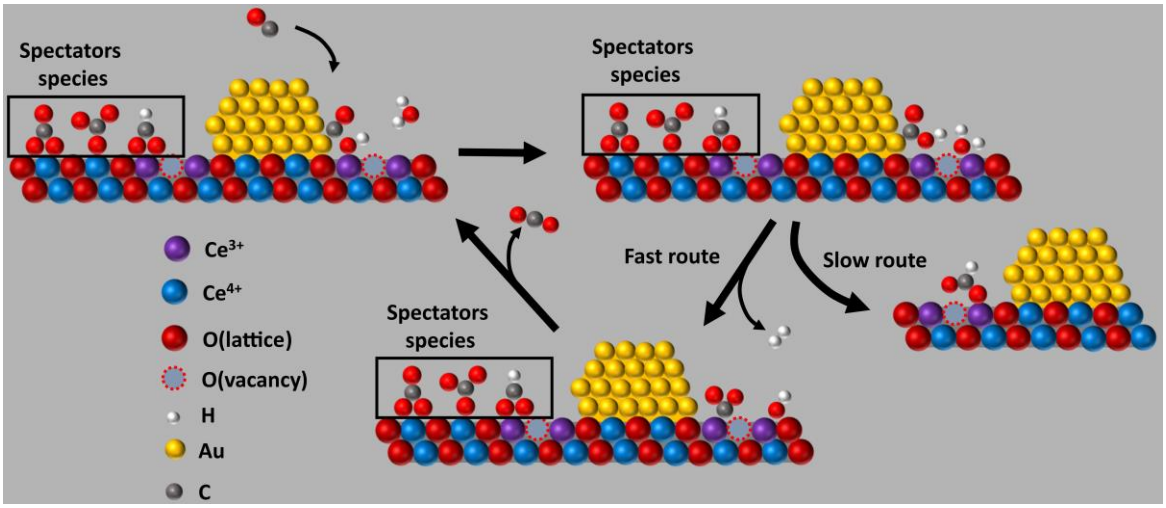

Scheme 1. Proposed low-temperature water gas shift reaction mechanism on Au/CeO_2 catalyst.

CONCLUSIONS

The use of in situ DRIFT spectroscopy combining steady-state, pulse of reactant and c-MES-PSD technique provides complementary information regarding the mechanism of the water gas shift reaction over an Au/CeO_2 catalyst. While in situ DRIFT is useful for characterizing stable surface species under steady-state conditions, time-resolved in situ IR spectroscopy is required to elucidate the dynamic of surface processes that occur during a solid catalyzed reaction. A CO Pulse under constant partial pressure of water is able to reduce Ce^{4+} to Ce^{3+}. However, formate and carbontate groups are accumulated on the surface but cannot be directly related to the CO_2 production. C-MES experimentation, coupled with processing the spectra with the PSD algorithm, allows the selective and sensitive identification of intermediate carbonaceous groups in the carbonate/formate region. It was demonstrated that the ceria support remains partially reduced under reaction and carbonate and most part of formate are reaction spectators. Moreover, carboxyl and carboxylate species were identified. Direct observation of these species has not been possible previously due to the highly overlapped bands in this spectral region. The c-MES results suggest that the low temperature WGS reaction proceed via a "associative mechanism", where monodente formate (m-HCOO) are a slower route, while carboxyl [C(O)OH] and carboxylate ($CO_2^{\delta-}$) species are in-phase with the production of CO_2 (fast route). This information is important for understanding the WGS reaction mechanism and can be used to design more efficient catalysts.

EXPERIMENTAL

Catalyst

Details of the material preparation methods have been previously reported [57]. Briefly, CeO_2 was prepared by precipitation in ammonia solution (pH 8.5) of $Ce(NO_3)_3{\cdot}6H_2O$ (99.99%, Sigma-Aldrich) dissolved in bi-distillated water. The gold supported catalyst was prepared by the method of deposition-precipitation method with urea (DPU) developed by Zanella et al. [58]. The metal dispersion was determined by high-resolution TEM (HRTEM) and high-angle annular dark field scanning transmission electron microscopy (HAADF-STEM). The catalytic activity of the catalysts for the water gas shift reaction was measured in a fixed-bed tubular reactor, i.d. = 4 mm (Supplementary Information).

DRIFT experiments

The water gas shift reaction on CeO_2 and Au/CeO_2 was investigated using a modified high-temperature Harrick DRIFT cell with ZnSe windows [59]. Time-resolved infrared spectra (up to 1 spectrum/0.39 s)

were recorded at a resolution of 1 or 4 cm^{-1} using an FTIR spectrometer (Thermo iS50 with a cryogenic MCT detector). To eliminate CO_2 and water vapor contributions to the spectra, the bench of the spectrometer and the optical path were continuously purged with purified air (Parker Balston FTIR purge gas generator). Gas flow was regulated using mass flow meters (Cole-Parmer). The entrance of the gases was controlled by a flow-through 10-ways valve electronically actuated (Vici-Valco) synchronized with the FTIR.

The cell was filled with 35-40 mg of the catalyst. The temperature of the catalyst was continuously monitored with a 1/32" thermocouple insert into the catalyst bed [60]. The catalyst was activated in situ at 523 K under oxidizing atmosphere, that is, 5% O_2/He flow (60 mL/min, 1h) and then purged under He flow (60 mL/min, 1h). Next, the catalyst was cooled down to 373 K and a reaction mixture with 1% CO and 2% H_2O composition was introduced into the DRIFT cell. IR spectra were collected between 373 and 623 K in steps of 50 K (remaining 1h at each temperature) during the WGS reaction. The desired concentration of water in He was obtained from a gas saturator filed with bi-distillated water immerse into a thermostatic bath. All the lines in contact with water were heated to prevent condensation.

Transition experiments were performed as follows. The Au/CeO_2 catalyst was exposed to a 2% H_2O current at 423 K for 1h. Next, a pulse of 5% CO (elapsed time = 10 s) was introduced, while maintaining the water current constant. IR spectra were taken at a velocity of 2.5 spectra/second.

Concentration-modulation excitation spectroscopy (c-MES) experiments were carried out by periodically switching between the reaction mixture (1% CO + 2% H_2O) to 2% H_2O/He (100cm^3/min) with a frequency (ω) of 8.3mHz into the DRIFT cell (square wave stimulation). The data was collected at a velocity of 0.25 spectra/second, and averaging 10 scans per spectra. The experimental set-up allows rapid exchange of gases, reaching the catalyst bed in less than 1 s, and the exchange of 98% of the gas composition occurs in less than 10 s [60].

Time-resolved spectra were further analysed using the phase sensitive detection (PSD) method developed by Baurcht and Fringeli [27]. This method is based on the perturbation of a system operating under steady state conditions (ss) by the periodic variation of an external parameter such as temperature, pressure or concentration of reactants. Therefore, all species in the system that are affected by the external parameter will change periodically with the same frequency as that of the disturbance, but with a phase delay (φ) [28,59]. A more sensible and selective analysis of the obtained information (spectra) can be achieved by demodulation of the oscillating response signal, A(t), as shown in Eq. (1):

$$A(\phi_k^{PSD}) = \frac{2}{T}\int_0^T A(t)\cdot \sin(k\cdot\omega\cdot t + \phi_k^{PSD})dt \qquad (1)$$

where, T is the length of one period, ω is the stimulation frequency, k is the demodulation index, ϕ^{PSD}_k is the demodulation phase angle for k·ω demodulation, and A(t) and A(ϕ^{PSD}) are the active species response in time- and phase-domain, respectively. In other words, the Eq. (1) transforms time-domain spectra, A(t), into phase-resolved spectra, $A_k(\phi^{PSD}_k)$. More details are provided in Supplementary Information.

The PSD method possess the following advantages: i) the spectra in the phase domain allows to distinguish and separate easily static signals from the changing ones, that is, spectator from active intermediate species; ii) the signal-to-noise (S/N) ratio in the spectra improves; and iii) the delays in the signals of different active species, which are due to the reaction mechanism, are better resolved in the phase-domain than in time-domain. The phase delays from different signals (e.g., intermediates species) determined by PSD, that is, the in-phase angle value of ϕ^{PSD} at which the amplitude reaches a maximum, contain kinetic information of the system, and the dynamic behaviour can be studied. Then, based on the φ values, species with different kinetics can be separated and insights into the catalytic mechanism can be addressed [28,61].

SUPPORTING INFORMATION

The authors have cited additional references within the Supporting Information.[62-74]

ACKNOWLEDGMENTS

The authors are grateful for the financial support from the Consejo Nacional de Investigaciones Científicas y Técnicas (CONICET) [Grant No. PIP-2022-08CO] and Agencia Nacional de Promoción de la Investigación, el Desarrollo Tecnológico y la Innovación (ANPCyT) [Grant Nos. PICT-2018-01332 and PICT-2020-03720]. The authors would also like to thank National University of Litoral for support in grant CAI+D PI 2020-058LI.

Keywords: carboxyl; carboxylate; cerium oxide; formate; gold catalysts; modulation spectroscopy

REFERENCES

[1] Q. Fu, H. Saltsburg, M. Flytzani-Stephanopoulos, *Science* **2003**, *301*, 935–938.

[2] J. A. Rodriguez, S. Ma, P. Liu, J. Hrbek, J. Evans, M. Pérez, *Science* **2007**, *318*, 1757–1760.

[3] R. Si, M. Flytzani-Stephanopoulos, *Angew. Chem.* **2008**, *120*, 2926–2929.

[4] A. Chen, X. Yu, Y. Zhou, S. Miao, Y. Li, S. Kuld, J. Sehested, J. Liu, T. Aoki, S. Hong, M. F. Camellone, S. Fabris, J. Ning, C. Jin, C. Yang, A. Nefedov, C. Wöll, Y. Wang, W. Shen, *Nat. Catal.* **2019**, *2*, 334–341.

[5] M. Nagao, Y. Suda, *Langmuir* **1989**, *5*, 42–47.

[6] M. Cargnello, V. V. T. Doan-Nguyen, T. R. Gordon, R. E. Diaz, E. A. Stach, R. J. Gorte, P. Fornasiero, C. B. Murray, *Science* **2013**, *341*, 771–773.

[7] X.-P. Fu, L.-W. Guo, W.-W. Wang, C. Ma, C.-J. Jia, K. Wu, R. Si, L.-D. Sun, C.-H. Yan, *J. Am. Chem. Soc.* **2019**, *141*, 4613–4623.

[8] M. Ziemba, J. Weyel, C. Hess, *Appl. Catal. B* **2022**, *301*, 120825.

[9] Y. Chen, H. Wang, R. Burch, C. Hardacre, P. Hu, *Faraday Discuss.* **2011**, *152*, 121–133.

[10] M. Ziemba, J. Weyel, C. Hess, *ACS Catal.* **2022**, *12*, 9503–9514.

[11] C. Ratnasamy, J. P. Wagner, *Catal. Rev.* **2009**, *51*, 325–440.

[12] C. M. Kalamaras, S. Americanou, A. M. Efstathiou, *J. Catal.* **2011**, *279*, 287–300.

[13] M. C. Ribeiro, G. Jacobs, L. Linganiso, K. G. Azzam, U. M. Graham, B. H. Davis, *ACS Catal.* **2011**, *1*, 1375–1383.

[14] T. Shido, Y. Iwasawa, *J. Catal.* **1992**, *136*, 493–503.

[15] G. Jacobs, L. Williams, U. Graham, D. Sparks, B. H. Davis, *J. Phys. Chem. B* **2003**, *107*, 10398–10404.

[16] R. Leppelt, B. Schumacher, V. Plzak, M. Kinne, R. Behm, *J. Catal.* **2006**, *244*, 137–152.

[17] A. Goguet, F. C. Meunier, D. Tibiletti, J. P. Breen, R. Burch, *J. Phys. Chem. B* **2004**, *108*, 20240–20246.

[18] F. C. Meunier, D. Tibiletti, A. Goguet, D. Reid, R. Burch, *Appl. Catal. A Gen.* **2005**, *289*, 104–112.

[19] X.-Q. Gong, P. Hu, R. Raval, *J. Chem. Phys.* **2003**, *119*, 6324–6334.

[20] Q. Wang, K. L. Yeung, M. A. Bañares, *J. Catal.* **2018**, *364*, 80–88.

[21] J. Graciani, K. Mudiyanselage, F. Xu, A. E. Baber, J. Evans, S. D. Senanayake, D. J. Stacchiola, P. Liu, J. Hrbek, J. F. Sanz, J. A. Rodriguez, *Science* **2014**, *345*, 546–550.

[22] K. Mudiyanselage, S. D. Senanayake, L. Feria, S. Kundu, A. E. Baber, J. Graciani, A. B. Vidal, S. Agnoli, J. Evans, R. Chang, S. Axnanda, Z. Liu, J. F. Sanz, P. Liu, J. A. Rodriguez, D. J. Stacchiola, *Angew. Chem. Int. Ed.* **2013**, *52*, 5101–5105.

[23] S. Aranifard, S. C. Ammal, A. Heyden, *J. Phys. Chem. C* **2014**, *118*, 6314–6323.

[24] N. C. Nelson, M.-T. Nguyen, V.-A. Glezakou, R. Rousseau, J. Szanyi, *Nat. Catal.* **2019**, *2*, 916–924.

[25] M. Jabłońska, *ChemCatChem* **2021**, *13*, 818–827.

[26] M. El-Roz, P. Bazin, M. Daturi, F. Thibault-Starzyk, *ACS Catal.* **2013**, *3*, 2790–2798.

[27] D. Baurecht, U. P. Fringeli, *Rev. Sci. Instrum.* **2001**, *72*, 3782–3792.

[28] A. Urakawa, T. Bürgi, A. Baiker, *Chem. Eng. Sci.* **2008**, *63*, 4902–4909.

[29] R. Leppelt, B. Schumacher, V. Plzak, M. Kinne, R. Behm, *J. Catal.* **2006**, *244*, 137–152.

[30] Q. Fu, A. Weber, M. Flytzani-stephanopoulos, *Catal. Lett.* **2001**, *77*, 87–95.

[31] D. Tibiletti, A. A.- Fonseca, R. Burch, Y. Chen, J. M. Fisher, A. Goguet, C. Hardacre, P. Hu, D. Thompsett, *J. Phys. Chem. B* **2005**, *109*, 22553–9.

[32] C. Schilling, C. Hess, *ACS Catal.* **2019**, *9*, 1159–1171.

[33] P. G. Lustemberg, M. V. Bosco, A. Bonivardi, H. F. Busnengo, M. V. Ganduglia-Pirovano, *J. Phys. Chem. C* **2015**, *119*, 21452–21464.

[34] R. Burch, A. Goguet, F. C. Meunier, *Appl. Catal. A Gen.* **2011**, *409–410*, 3–12.

[35] C. Binet, M. Daturi, J.-C. Lavalley, *Catal. Today* **1999**, *50*, 207–225.

[36] G. Finos, S. Collins, G. Blanco, E. del Rio, J. M. Cíes, S. Bernal, A. Bonivardi, *Catal. Today* **2012**, *180*, 9–18.

[37] A. Fielicke, G. von Helden, G. Meijer, B. Simard, D. M. Rayner, *J. Phys. Chem. B* **2005**, *109*, 23935–23940.

[38] A. S. Wörz, U. Heiz, F. Cinquini, G. Pacchioni, *J. Phys. Chem. B* **2005**, *109*, 18418–18426.

[39] T. Tabakova, F. Boccuzzi, M. Manzoli, J. W. Sobczak, V. Idakiev, D. Andreeva, *Appl. Catal. A Gen.* **2006**, *298*, 127–143.

[40] A. Fielicke, G. von Helden, G. Meijer, D. B. Pedersen, B. Simard, D. M. Rayner, *J. Am. Chem. Soc.* **2005**, *127*, 8416–8423.

[41] S. E. Collins, J. M. Cíes, E. del Río, M. López-Haro, S. Trasobares, J. J. Calvino, J. M. Pintado, S. Bernal, *J. Phys. Chem. C* **2007**, *111*, 14371–14379.

[42] J. M. Cíes, E. del Río, M. López-Haro, J. J. Delgado, G. Blanco, S. Collins, J. J. Calvino, S. Bernal, *Angew. Chem. Int. Ed.* **2010**, *49*, 9744–9748.

[43] C. Binet, A. Badri, J.-C. Lavalley, *J. Phys. Chem.* **1994**, *98*, 6392–6398.

[44] J. Vecchietti, S. Collins, W. Xu, L. Barrio, D. Stacchiola, M. Calatayud, F. Tielens, J. J. Delgado, A. Bonivardi, *J. Phys. Chem. C* **2013**, *117*, 8822–8831.

[45] C. Binet, M. Daturi, J.-C. Lavalley, *Catal Today* **1999**, *50*, 207–225.

[46] J. Vecchietti, A. Bonivardi, W. Xu, D. Stacchiola, J. J. Delgado, M. Calatayud, S. E. Collins, *ACS Catal.* **2014**, *4*, 2088–2096.

[47] A. Davydov, *Molecular Spectroscopy of Oxide Catalyst Surfaces*, John Wiley & Sons, Ltd., Chichester, **2003**, p. 135.

[48] D. H. Gibson, *Coord. Chem. Rev.* **1999**, *185–186*, 335–355.

[49] F. C. Meunier, R. Kdhir, N. Potrzebowska, N. Perret, M. Besson, *Inorg. Chem.* **2019**, *58*, 8021–8029.

[50] M. Raphulu, J. McPherson, E. van der Lingen, J. A. Anderson, M. S. Scurrell, *Gold. Bull.* **2010**, *43*, 334–344.

[51] K. R. Lane, L. Sallans, R. R. Squires, *Inorg. Chem.* **1984**, *23*, 1999–2000.

[52] D. J. Darensbourg, A. Rokicki, M. Y. Darensbourg, *J. Am. Chem. Soc.* **1981**, *103*, 3223–3224.

[53] S. W. Lee, W. D. Tucker, M. G. Richmond, *Inorg. Chem.* **1990**, *29*, 3053–3056.

[54] D. Forney, M. E. Jacox, W. E. Thompson, *J. Chem. Phys.* **2003**, *119*, 10814–10823.

[55] T. E. Shubina, C. Hartnig, M. T. M. Koper, *Phys. Chem. Chem. Phys.* **2004**, *6*, 4215.

[56] S. D. Senanayake, P. J. Ramírez, I. Waluyo, S. Kundu, K. Mudiyanselage, Z. Liu, Z. Liu, S. Axnanda, D. J. Stacchiola, J. Evans, J. A. Rodriguez, *J. Phys. Chem. C* **2016**, *120*, 1778–1784.

[57] J. Vecchietti, S. Collins, J. J. Delgado, M. Małecka, E. Rio, X. Chen, S. Bernal, A. Bonivardi, *Top. Catal.* **2011**, *54*, 201–209.

[58] R. Zanella, S. Giorgio, C. R. Henry, C. Louis, *J. Phys. Chem. B* **2002**, *106*, 7634–7642.

[59] A. Aguirre, S. E. Collins, *Catal. Today* **2013**, *205*, 34–40.

[60] A. Aguirre, S. E. Collins, *Mol. Catal.* **2020**, *481*, 100628.

[61] P. D. Srinivasan, B. S. Patil, H. Zhu, J. J. Bravo-Suárez, *React. Chem. Eng.* **2019**, *4*, 862–883.

[62] N. Hassler, D. Baurecht, G. Reiter, U. P. Fringeli, *J. Phys. Chem. C* **2011**, *115*, 1064–1072.

[63] G. Kresse, J. Hafner, *Phys. Rev. B* **1994**, *49*, 14251–14269.

[64] G. Kresse, J. Furthmüller, *Phys. Rev. B* **1996**, *54*, 11169–11186.

[65] G. Kresse, J. Hafner, *Phys. Rev. B* **1993**, *47*, 558–561.

[66] P. E. Blöchl, *Phys. Rev. B* **1994**, *50*, 17953–17979.

[67] G. Kresse, J. Hafner, *J. Phys. Condens. Matter* **1994**, *6*, 8245–8257.

[68] G. Kresse, D. Joubert, *Phys. Rev. B* **1999**, *59*, 1758–1775.

[69] S. L. Dudarev, G. A. Botton, S. Y. Savrasov, C. J. Humphreys, A. P. Sutton, *Phys. Rev. B* **1998**, *57*, 1505–1509.

[70] J. P. Perdew, K. Burke, M. Ernzerhof, *Phys. Rev. Lett.* **1997**, *78*, 1396–1396.

[71] S. Bhasker-Ranganath, M. S. Rahman, C. Zhao, F. Calaza, Z. Wu, Y. Xu, *ACS Catal.* **2021**, *11*, 8621–8634.

[72] H. J. Monkhorst, J. D. Pack, *Phys. Rev. B* **1976**, *13*, 5188–5192.

[73] S. Grimme, J. Antony, S. Ehrlich, H. Krieg, *J. Chem. Phys.* **2010**, *132*, 154104.

[74] S. Grimme, *J. Comput. Chem.* **2006**, *27*, 1787–1799.

TABLE OF CONTENT

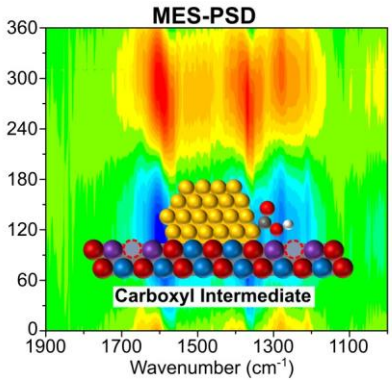

Modulated experiments (MES-PSD) by diffuse reflectance infrared (DRIFT) spectroscopy allowed identification of carboxyl species as a key intermediate during WGS reaction over Au/CeO_2 catalyst.

https://twitter.com/intec_ok